Pulling Tethers from Pore-Spanning Bilayers: Towards Simultaneous Determination of Local Bending Modulus and Lateral Tension of Membranes

*Marta Kocun and Andreas Janshoff**

Membrane mechanics play a pivotal role in many cellular processes, such as endocytosis, exocytosis comprising the budding–fission–fusion chain of events, cell migration, and cell division.[1] A fundamental understanding of these intricate processes that involve bending deformation, shearing, and area dilatation of the plasma membrane requires detailed knowledge of mechanical parameters on various length scales ranging from the dimension of the entire cell (5–20 μm) to the mesh size of the underlying cytoskeleton (30–300 nm). However, the complicated and intrinsically heterogeneous composition of native plasma membranes that may consist of thousands of different lipids, steroids, and proteins as well as the attachment of the lipid bilayer to the underlying cytoskeleton render the accurate determination of elastic constants a difficult task. Therefore, tailored giant liposomes that allow for the control of membrane composition have been frequently used as model systems to measure mechanical parameters of lipid bilayers, such as area compressibility and bending moduli. Because lipid bilayers are extremely flexible, the bending rigidity measurements are frequently inferred indirectly from bilayer fluctuations using optical microscopy.[2] The measurements either utilize the dependence of thermally excited membrane undulations on membrane rigidity or determine directly the force needed to deform a lipid bilayer concomitant to its shape. The former approach is realized by directly observing the fluctuations through flicker spectroscopy using optical microscopy and suppressing fluctuations in the low-tension regime of a micropipette suction experiment.[2b–d] The latter—a direct determination of the bending rigidity—might be achieved by estimating the force needed to pull highly curved nanotubes (tethers) out of membranes.[1j,2a,2e,3] Formation of membrane-tethers requires work against bending and against the creation of new surface producing a constant force to further elongate the nanotube ($F \approx \sqrt{\sigma\kappa}$).[2f,3b] Separation of surface tension σ and bending modulus κ requires sophisticated experiments, as recently accomplished by Cuvelier et al. using a combination of micropipette manipulation and optical tweezers techniques.[2e]

Dr. M. Kocun, Prof. A. Janshoff
Institute of Physical Chemistry
University of Goettingen
Tammannstr. 6, 37077 Goettingen, Germany
E-mail: Andreas.Janshoff@chemie.uni-goettingen.de

DOI: 10.1002/smll.201101557

So far, none of the techniques employing giant liposomes are suitable to access and map local bending moduli. Therefore, a new model system—pore-spanning membranes—was envisioned that would combine the merits of giant liposomes with those of solid supported bilayers.[4] Fluid membranes were prepared on a porous matrix, which allows for the investigation of the local mechanical properties of bilayers that are essentially elastically decoupled by the underlying porous mesh. The individual membranes are easily accessible by atomic force microscopy, which is well-suited for local mapping of mechanical properties.[4c,4f] Although the approach has many advantages over conventional liposome-based models of the biomembrane, a quantitative unequivocal measurement of bending moduli by means of indentation measurements remains hardly attainable since the elastic response upon indentation is mainly governed by the lateral tension produced by adhesion of the bilayer on the pore rims, while bending plays a minor role unless the pores become very small.[4c,4f,4h,5]

In this work we demonstrate how the bending modulus κ and the lateral tension σ of a membrane can be determined locally at the same spot by recording a single force cycle with a conventional atomic force microscope. **Figure 1**a illustrates the preparation protocol of fluid pore-spanning bilayers derived from giant liposomes deposited on mercaptoethanol functionalized gold-coated silicon nitride substrates (Figure 1b), as introduced recently.[4c] Porous silicon nitride with pore diameter 1.2 μm is ideally suited to combine epifluorescence with scanning probe microscopy. The individual pore-spanning membranes composed of POPC labeled with Texas-Red DHPE can be easily visualized by fluorescence microscopy (Figure 1c) in order to perform site-specific force experiments by atomic force microscopy. Figure 1c shows individually spread giant liposomes with their typical heart-shape on the porous support (pore radius 600 nm). Only the free-standing bilayer produces fluorescence since emission is quenched on the gold-covered pore rims.

The basic principle of the measurement to simultaneously determinate lateral tension σ and bending modulus κ of pore-spanning lipid bilayers is illustrated in **Figure 2**a–c. It relies on a combination of bilayer indentation upon approach of the cantilever, providing an estimate for the lateral tension and subsequent tether formation upon retraction from which the bending modulus can be inferred if σ is known. A typical force cycle obtained from indenting a pore spanning bilayer (light gray) followed by pulling a tether (membrane-nanotube)

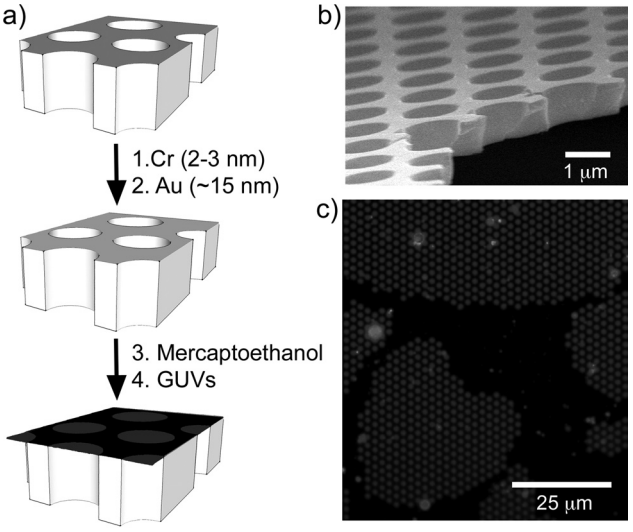

Figure 1. a) Scheme illustrating preparation of fluid, pore-spanning lipid bilayers from giant liposomes. Porous silicon nitride substrate is coated first with chromium to enhance adhesion followed by a thin gold layer that is subsequently functionalized with mercaptoethanol. Giant liposomes adhere and spread on these substrates forming free-standing bilayers with preserved fluidity. b) Scanning electron micrograph of the porous substrate. c) Fluorescence micrograph of pore spanning POPC bilayers after spreading and rupturing of giant liposomes doped with TexasRed-DHPE.

out of the membrane (dark blue) is shown in Figure 2d. The jump to the baseline corresponds to stochastic rupture of the tether. The apparent spring constant k_{app} of the free-standing bilayer can be estimated from the linear slope (black line) of the force-indentation curve after contact of the indenter with the bilayer (light gray), while the tether force is identical to the force plateau (black lines) upon retraction of the cantilever (dark gray).

Indentation of the bilayers covering micrometer-sized pores allows for the determination of the lateral tension without interference from bending or stretching, as previously investigated in great detail.[4c] We propose that in-plane area dilatation of the bilayer does not significantly contribute to the bilayer's elastic response upon indentation. Indentation causes the membrane to rather flow into the pore, while the loss in free energy concomitant with the production of excess membrane area not attached to the pore rims creates a tension that gives rise to the measured restoring force. Therefore, the resistance to production of free-standing area originates from adhesion of the bilayer to the rim. We can exclude stretching, i.e., area dilatation ($\tau = K_a \frac{\Delta A}{A_0}$, with A_0 the membrane area prior to indentation, τ the stress tensor, ΔA the change in area, and K_a the area compressibility), of the pore-spanning bilayer upon indentation since it would produce a nonlinear force response ($F = \int \tau dA \sim h^3$) with indentation depth h.[4i] In contrast, we exclusively found a linear response ($F \propto h$) upon indentation, which is indicative of a tension-dominated response. The absence of stretching is attributed to the existence of a membrane reservoir preventing the laterally highly incompressible membrane from being dilated in-plane. This is further supported by the circumstance that a phospholipid membrane in

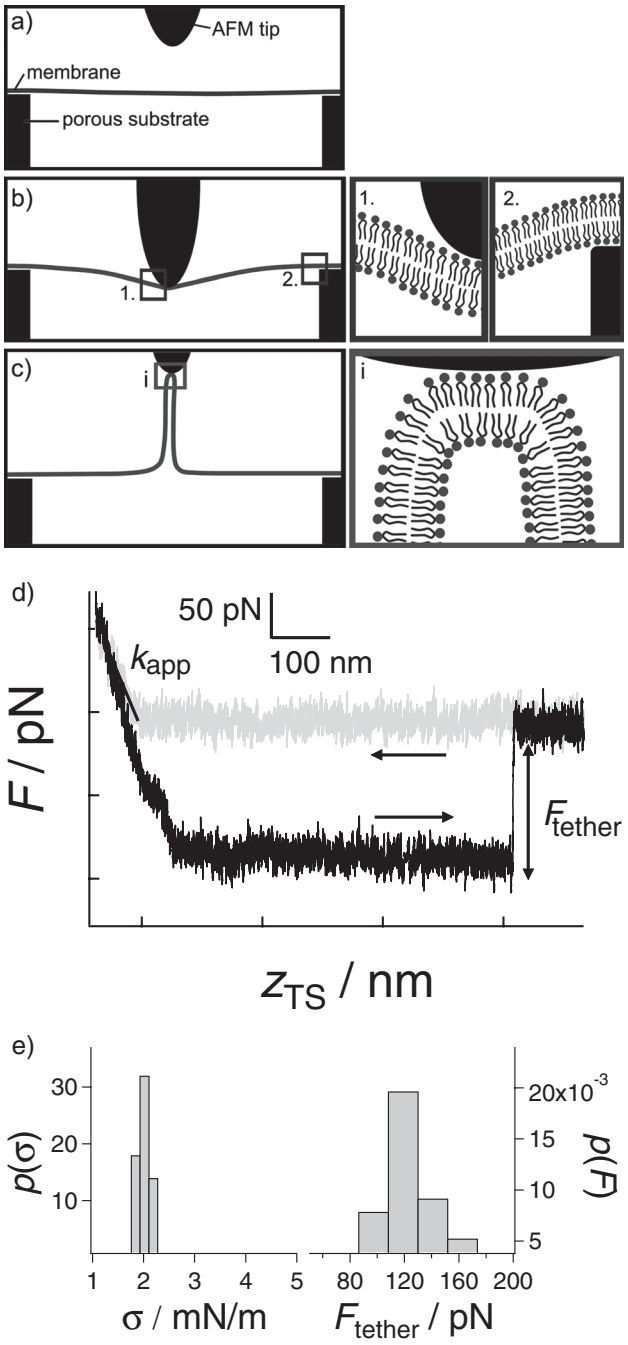

Figure 2. a–c) Measurement principle to obtain the local bending modulus of a lipid bilayer by first indenting a pore spanning membrane (b) and subsequently, within the same force cycle, pulling a tether away from the surface (c). d) Typical force separation curve showing a linear force response upon indentation of the pore-spanning membrane (light gray) and formation of a nanotube upon retraction (dark gray) giving rise to a constant force plateau (F_{tether}). The black lines denote the determination of k_{app} and F_{tether}. e) Histograms of lateral tension σ and tether force F_{tether} obtained from force cycles on pure POPC.

the fluid state cannot withstand an area dilatation $\frac{\Delta A}{A_0} \geq 5\%$. However, we could easily indent the membrane into the pore by far more than 5% area gain and never recorded any rupture events in the force indentation curve, as verified independently by fluorescence microscopy after the force measurements.

NANO MICRO small

Bending of the bilayer can also be excluded as a major source of force against indentation. This can be rationalized by comparing the obtained experimental value for the apparent spring constant k_{app}, i.e. the slope upon indentation, with the expected theoretical spring constant produced solely by bending of the pore-covering bilayer with a point-like indenter ($k_{app}^{bend} = {4\pi E d^3}/{3(1-\nu^2)R_{pore}^2}$, with Young's modulus E, the Poisson ratio ν, the thickness of the bilayer d, and the pore radius R_{pore}).[4f] Assuming reasonable values for E such as 28 MPa, $\nu = 0.33$, and a thickness of $d = 5.5$ nm, which corresponds to a bending modulus of $\kappa = 1.1 \times 10^{-19}$ J for the membrane, we obtain a theoretical apparent spring constant of the bilayer $k_{app}^{bend} \approx 4 \times 10^{-5}$ N m^{-1}. In contrast, we find experimental values for k_{app} in the range of (0.1 to 5) $\times 10^{-3}$ N m^{-1} depending on lipid composition (vide infra). Therefore, we can safely exclude bending as the major contribution to the restoring force upon indentation. Notably, an apparent spring constant well below 0.01 mN m^{-1} could hardly be detected by force spectroscopy carried out with an AFM due to the limited force resolution of 5–10 pN. A more thorough computation employing the exact indenter geometry confirms this finding.[4f,4h,6]

From this chain of arguments, we conclude that lateral tension σ produced by adhesion of the bilayer to the rim governs the elastic response upon indentation. Computing σ from Young–Laplace's law ($F = \pi R_1^2 \Delta P = \pi\sigma R_1^2(R_1^{-1} + R_2^{-1}) = \pi\sigma R_1 = \pi\sigma\tan(\alpha)h$, with ΔP the pressure difference between inside and outside, and, R_1 and R_2 the principal radii of curvature) assuming a conical indenter in conformal contact with the membrane provides $\sigma = k_{app}\cot(\alpha)/\pi \approx k_{app}$, with the opening angle $\alpha = 17.5°$ of the cone. The obtained σ-values are essentially identical with those obtained from an asymptotic fit of the force-indentation curve using ($h = F(4\pi\sigma)^{-1}[1 - \ln(FR_{tip}(2\pi\sigma R_{pore}^2)^{-1})]$) as recently described for indentation of pore spanning bilayer in the absence of bending.[4h,6]

A contact time between tip and pore spanning membrane of 5 s at 100 pN load force is sufficient to produce enough non-specific adhesion between tip and bilayer that tethers can be pulled upon retraction of the cantilever from the surface. The tether force F_{tether} is related to the product of lateral tension σ and bending modulus κ according to Equation 1:

$$F_{tether} = 2\pi\sqrt{2\sigma\kappa} + 2\pi\eta_{app}v/C \quad (1)$$

η_{app} denotes the apparent membrane viscosity, C a correction factor ($C = 1.6$), and v the pulling velocity.[1j,7] Notably, neither the slope upon indentation nor the tether force turned out to be dependent on the pulling velocity as suggested by Equation 1. The intrinsic inter-bilayer friction would be orders of magnitude smaller and therefore not measurable by atomic force spectroscopy.[8] According to Turner et al., and Maeda et al., as well as our own experiments and calculations, dissipation contributes to the tether force in a negligible fashion (around 0.1 fN), which is well below the force resolution of the AFM (5 pN).[3d,9] Also, the lateral diffusion constant of the pore spanning lipids did not deviate from the mobility of lipids in GUVs, ruling out an appreciable contribution from friction between the bilayer and the pore rims.[4c] Figure 2e shows two normalized histograms of the lateral tension and the tether force obtained from a number of force cycles ($n > 50$) on pure pore-spanning POPC bilayers. Notably, only nanotubes that display a constant force were considered since initiation of membrane-tethers involves a nonlinear increase followed by slight overshoot of force. Plateau forces were usually noted when the tether-extension goes beyond 50 nm.

The feasibility of our approach to locally determine the bending modulus of free-standing membranes is demonstrated by using three different lipid compositions that exhibit a considerable spread in bending modulus without entering the gel phase. We prepared GUVs from pure POPC and a POPC/cholesterol (3:1) mixture that is expected to exhibit a significantly higher bending rigidity. Furthermore, we also softened an existing bilayer by addition of isopropanol (0.67 M, POPC/isopropanol) which should lower lateral tension and bending modulus. **Figure 3** shows two typical force–separation curves obtained from POPC/isopropanol (**1**) and POPC/cholesterol (**2**) pore-spanning bilayers. Both, the lateral tension of the bilayer and the corresponding tether force are substantially larger for POPC/cholesterol in comparison to POPC or POPC/isopropanol bilayers. Computation of the bending moduli for all three bilayer types according to Equation 1 is summarized in **Table 1**. For a pure POPC bilayer we determined an average bending modulus of (6.7 ± 2.0) $\times 10^{-20}$ J. This value is in good agreement with literature values ranging from (0.77 to 1.6) $\times 10^{-19}$ J.[2b,10]

Interestingly, we found that membranes prepared from pure lipids such as POPC or DOPC exhibit a very narrow distribution of tension values, while addition of cholesterol (30 mol-%) broadens the histogram considerably (see the Supporting Information). This might reflect the intrinsic

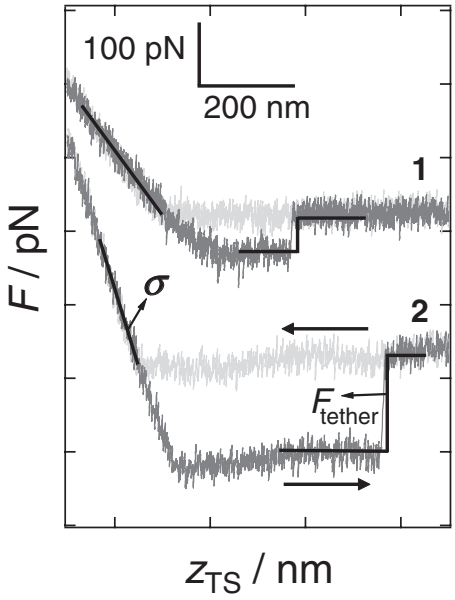

Figure 3. Two typical force curves obtained from POPC membranes exposed to 0.67 M isopropanol (**1**) and POPC/cholesterol (3:1) (**2**) are shown. Indentation (light gray) reveals a linear slope (black line) governed by lateral tension of the bilayers, while tether formation (dark gray) is represented by a constant tether force (black line).

Table 1. Summary of measured lateral tension σ, tether force F_{tether} obtained from Gaussian fits of the corresponding histograms, and computed bending modulus κ (Equation 1).

Lipid Composition	σ [mN m^{-1}]	F_{tether} [pN]	κ [10^{-20} J]
POPC	2.4 ± 0.5	112 ± 2	6.7 ± 2.0
POPC/isop.	0.86 ± 0.13	43 ± 1	2.8 ± 3.0
POPC/chol.	2.6 ± 0.9	134 ± 1	8.7 ± 3.0

heterogeneity of the bilayer and the impact of cholesterol on adhesion of the bilayer to the pore rims. Notably, the accuracy of the bending modulus obtained from Equation 1 is mainly limited by the force resolution of the AFM, since $\Delta\kappa \approx \frac{F_{tether}}{2\pi\sigma}\Delta F_{tether}$.

The bending moduli of all three systems agree well with those reported in the literature. As expected, we found a small but significant increase in κ by addition of cholesterol. It is well-known that cholesterol enhances the ordering of the lipids and therefore increases the bending modulus of the membrane.[2b,10b–d] For instance, addition of cholesterol to fluid DMPC (dimyristoylphosphatidylcholine) bilayers increases the bending modulus from (1.3 to 4.1) × 10^{-19} J. Ipsen et al. recently reported on an increase of κ from 1.6 × 10^{-19} J for pure POPC to 3.5 × 10^{-19} J for POPC/cholesterol (3:1) using a micropipette aspiration technique.[10c] Employing a combination of dynamic light scattering and neutron spin echo experiments Arriaga et al. found a bending modulus of 0.77 × 10^{-19} J for pure POPC vesicles and 1.11 × 10^{-19} J for POPC with 40 mol-% cholesterol, which is in very good agreement with our findings.[10d]

In contrast, exposure to small-chain alcohols reduces both, lateral tension and bending modulus.[4c,10e] We explain the reduction of σ by the partitioning of isopropanol into the bilayer thus releasing some of the pre-stress in the bilayer. Ly and Longo found that the bending modulus of SOPC (1-stearoyl-2-oleoyl-phosphatidylcholine) decreases from 8.3 × 10^{-20} J to 4.3 × 10^{-20} J as the short-chain alcohol concentration saturates.[10e] This is in good agreement with earlier findings of Safinya et al. who investigated the impact of pentanol on the bending modulus of fluid DMPC.[11] It is the reduction of interfacial tension γ, due to partitioning of the alcohol into the bilayer, that is responsible for this trend which is proportional to the area compressibility $K_a \sim \gamma$ and through the bilayer thickness d also to the bending modulus $\kappa \sim K_a d^2$.

Although it is in principle conceivable to obtain both bending modulus and lateral tension from indenting free-standing membranes over very small pores ($R_{pore} < 30$ nm), the requirement of exactly indenting the bilayer in the center of the pore is difficult to fulfill. Even small deviations from the center increase the apparent stiffness of the bilayer. It is, however, extremely difficult to perform the indentation experiment directly in the center of the pore due to the inevitable thermal drift of the instrument. In contrast, using larger pores in which tension governs the elastic response to indentation the exact location of the indenter on pore is less important.

In conclusion, we established a new method that allows determination of the lateral tension and the bending moduli of membranes within a single force cycle. The experimental cycle is composed of indentation used to determine the tension of the bilayer and originates from preferred rim-adhesion followed by nanotube formation that provides a constant tether force, which depends on the product of bending modulus and tension. Our method allows investigating a wide range of bending moduli from 10–100 k_BT and lateral tensions ranges from 0.05 mN m^{-1} to essentially bilayer lysis.

It is only this combination of indentation and pulling that permits maps of bending moduli to be obtained, allowing identification of regions of high and low lipid ordering. This is primarily due to the elastic decoupling of the individual pores. Depending on the mesh size of the porous support, the mechanical properties of domains within phase separated membranes become accessible. This will allow us to draw a more comprehensive picture of membrane mechanics on a local scale.

Experimental Section

Materials: 1-Palmitoyl-2-oleoyl-*sn*-glycero-3-phosphocholine (POPC), 1,2-dioleoyl-*sn*-glycero-3-phosphocholine (DOPC) was purchased from Avanti Polar Lipids (Alabaster, AL), cholesterol was obtained from Sigma-Aldrich (Steinheim, Germany). Membranes were labeled (0.1 mol-%) with sulforhodamine-1,2-dihexanoyl-*sn*-glycero-3-phosphoethanolamine (TexasRed-DHPE, Sigma-Aldrich). Mercaptoethanol (Sigma-Aldrich) and propan-2-ol (VWR, Fontenay-sous-Bois, France) were used as purchased. Water used in preparation of buffers was filtered by a Millipore system (Milli-Q System from Millipore, Molsheim, France; resistance >18 MΩ cm^{-1}).

Vesicle Preparation: Giant unilamellar vesicles (GUVs) were prepared by electroformation as previously described.[4c] 50 µL of 1 mg mL^{-1} lipid solution was spread uniformly on indium tin oxide (ITO) slides and subsequently dried under vacuum for at least 3 h at 64 °C. Two opposing ITO slides were connected to a waveform generator producing an alternating voltage at 12 Hz. Voltage was increased every 60 s from 0.05 to 0.2 V in increments of 0.01 V. The increments were then enlarged to 0.1 V until the final voltage of 1.6 V was reached (total duration: 3 h). Finally, a square 5 Hz wave was applied for 5 min.

Porous Substrates: Silicon nitride substrates with pore radii of 600 nm were purchased from Fluxxion B.V. (Eindhoven, The Netherlands). The porous substrates were coated with a 2–3 nm thick layer of chromium followed by a 10–15 nm thick layer of gold (Bal-Tec MCS610 evaporator). The gold-coated substrates were subsequently oxygen-plasma (1 min) and argon-plasma (1 min) treated and placed in a 20 mM ethanolic mercaptoethanol self-assembly solution for 1 h.

Pore-Spanning Membranes: Functionalized porous substrates were placed in a homemade Teflon holder filled with ethanol. Ethanol was replaced by phosphate-buffered saline (PBS: 20 mM NaH_2PO_4/Na_2HPO_4, 100 mM NaCl, pH 7.4), and 20 µL of GUVs were added. GUVs sedimented to the surface and immediately spread to create lipid bilayer patches.

Atomic Force Microscopy (AFM): AFM imaging and force indentation curve acquisition was performed in PBS buffer with a MFP-3D (Asylum Research, Santa Barbara, CA) and silicon nitride AFM probes (MLCT-AU type, 310 µm long C lever) purchased from Bruker AFM Probes (Mannheim, Germany). The spring constants were calibrated as recently described.[4c]

NANO MICRO small

Fluorescence Microscopy: An Olympus BX-51 upright optical microscope (Olympus Germany GmbH, Hamburg, Germany) was used equipped with filters for TexasRed and BODIPY fluorescence (UMNG2 and UMNB2, Olympus Germany GmbH, Hamburg, Germany) and immersion objectives with 40× (Olympus, LUMPlanFL 40×, N.A. = 0.8) and 100× (Olympus, LUMPlanFL 100×, N.A. = 1.00) magnifications.

Supporting Information

Supporting Information is available from the Wiley Online Library or from the author.

Acknowledgements

The authors gratefully acknowledge financial support by the DFG (JA 963 8-1) and a fellowship from the International Max Planck Graduate School of Biophysics and Complex Systems (MK).

[1] a) K. E. Gottschalk, J. Schmitz, *Soft Matter* **2008**, *4*, 1373; b) N. Gov, *Nat. Mater.* **2011**, *10*, 412; c) J. Guck, F. Lautenschlager, S. Paschke, M. Beil, *Integr. Biol.* **2010**, *2*, 575; d) J. F. Joanny, J. Y. Tinevez, U. Schulze, G. Salbreux, J. Roensch, E. Paluch, *Proc. Natl. Acad. Sci. USA* **2009**, *106*, 18581; e) L. Johannes, S. Mayor, *Cell* **2010**, *142*, 507; f) S. Kumar, T. P. Lele, *Cell Biochem. Biophys.* **2007**, *47*, 348; g) A. Pietak, S. D. Waldman, *Phys. Biol.* **2008**, *5*; h) S. Suresh, *Acta Biomater.* **2007**, *3*, 413; i) A. P. Zhu, N. Fang, *Biomacromolecules* **2005**, *6*, 2607; j) M. P. Sheetz, *Nat. Rev. Mol. Cell Biol.* **2001**, *2*, 392.

[2] a) L. Bo, R. E. Waugh, *Biophys. J.* **1989**, *55*, 509; b) E. Evans, W. Rawicz, *Phys. Rev. Lett.* **1990**, *64*, 2094; c) D. V. Zhelev, D. Needham, R. M. Hochmuth, *Biophys. J.* **1994**, *67*, 720; d) H. G. Dobereiner, G. Gompper, C. K. Haluska, D. M. Kroll, P. G. Petrov, K. A. Riske, *Phys. Rev. Lett.* **2003**, *91*; e) D. Cuelier, D. I. P. Bassereau, P. Nassoy, *Biophys. J.* **2005**, *88*, 2714; f) V. A. Harmandaris, M. Deserno, *J. Chem. Phys.* **2006**, *125*.

[3] a) R. E. Waugh, R. M. Hochmuth, *Biophys. J.* **1987**, *52*, 391; b) R. M. Hochmuth, W. D. Marcus, *Biophys. J.* **2002**, *82*, 2964; c) B. G. Hosu, M. Sun, F. Marga, M. Grandbois, G. Forgacs, *Phys. Biol.* **2007**, *4*, 67; d) J. W. Armond, J. V. Macpherson, M. S. Turner, *Langmuir* **2011**, *27*, 8269; e) B. Pontes, N. B. Viana, L. T. Salgado, M. Farina, V. Moura Neto, H. M. Nussenzveig, *Biophys. J.* **2011**, *101*, 43.

[4] a) C. Hennesthal, J. Drexler, C. Steinem, *ChemPhysChem* **2002**, *3*, 885; b) C. Hennesthal, C. Steinem, *J. Am. Chem. Soc.* **2000**, *122*, 8085; c) M. Kocun, T. D. Lazzara, C. Steinem, A. Janshoff, *Langmuir* **2011**, *27*, 7672; d) M. Kocun, W. Mueller, M. Maskos, I. Mey, B. Geil, C. Steinem, A. Janshoff, *Soft Matter* **2010**, *6*, 2508; e) B. Lorenz, I. Mey, S. Steltenkamp, T. Fine, C. Rommel, M. M. Muller, A. Maiwald, J. Wegener, C. Steinem, A. Janshoff, *Small* **2009**, *5*, 832; f) I. Mey, M. Stephan, E. K. Schmitt, M. M. Muller, M. Ben Amar, C. Steinem, A. Janshoff, *J. Am. Chem. Soc.* **2009**, *131*, 7031; g) I. Ortega-Blake, E. Ovalle-Garcia, J. J. Torres-Heredia, A. Antillon, *J. Phys. Chem. B* **2011**, *115*, 4826; h) S. Steltenkamp, M. M. Muller, M. Deserno, C. Hennesthal, C. Steinem, A. Janshoff, *Biophys. J.* **2006**, *91*, 217; i) S. Scheuring, R. P. Goncalves, G. Agnus, P. Sens, C. Houssin, B. Bartenlian, *Nat. Methods* **2006**, *3*, 1007.

[5] a) M. Arnoldi, M. Fritz, E. Bauerlein, M. Radmacher, E. Sackmann, A. Boulbitch, *Phys. Rev. E* **2000**, *62*, 1034; b) A. A. Boulbitch, *Phys. Rev. E* **1998**, *57*, 2123; c) R. Merkel, R. Simson, D. A. Simson, M. Hohenadl, A. Boulbitch, E. Wallraff, E. Sackmann, *Biophys. J.* **2000**, *79*, 707.

[6] D. Norouzi, M. M. Muller, M. Deserno, *Phys. Rev. E* **2006**, *74*.

[7] a) R. M. Hochmuth, H. C. Wiles, E. A. Evans, J. T. Mccown, *Biophys. J.* **1982**, *39*, 83; b) D. J. Muller, M. Krieg, J. Helenius, C. P. Heisenberg, *Angew. Chem., Int. Ed.* **2008**, *47*, 9775; c) B. Lorenz, R. Keller, E. Sunnick, B. Geil, A. Janshoff, *Biophys. Chem.* **2010**, *150*, 54.

[8] E. A. Evans, R. M. Hochmuth, *Biophys. J.* **1976**, *16*, 1.

[9] N. Maeda, T. J. Senden, J. M. di Meglio, *Biochim. Biophys. Acta, Biomembr.* **2002**, *1564*, 165.

[10] a) J. R. Henriksen, J. H. Ipsen, *Eur. Phys. J. E* **2004**, *14*, 149; b) J. Henriksen, A. C. Rowat, J. H. Ipsen, *Eur. Biophys. J. Biophy.* **2004**, *33*, 732; c) J. Henriksen, A. C. Rowat, E. Brief, Y. W. Hsueh, J. L. Thewalt, M. J. Zuckermann, J. H. Ipsen, *Biophys. J.* **2006**, *90*, 1639; d) L. R. Arriaga, I. Lopez-Montero, F. Monroy, G. Orts-Gil, B. Farago, T. Hellweg, *Biophys. J.* **2009**, *96*, 3629; e) H. V. Ly, M. L. Longo, *Biophys. J.* **2004**, *87*, 1013.

[11] C. R. Safinya, E. B. Sirota, R. F. Bruinsma, C. Jeppesen, R. J. Plano, L. J. Wenzel, *Science* **1993**, *261*, 588.

Received: August 1, 2011
Revised: October 31, 2011
Published online: January 9, 2012

